

SCIENTIFIC REPORTS

OPEN

Relation between the Co-O bond lengths and the spin state of Co in layered Cobaltates: a high-pressure study

Yi-Ying Chin¹, Hong-Ji Lin¹, Zhiwei Hu², Chang-Yang Kuo², Daria Mikhailova^{2,3,4}, Jenn-Min Lee¹, Shu-Chih Haw¹, Shin-An Chen¹, Walter Schnelle², Hirofumi Ishii¹, Nozomu Hiraoka¹, Yen-Fa Liao¹, Ku-Ding Tsuei¹, Arata Tanaka⁵, Liu Hao Tjeng², Chien-Te Chen¹ & Jin-Ming Chen¹

The pressure-response of the Co-O bond lengths and the spin state of Co ions in a hybrid 3d-5d solid-state oxide $\text{Sr}_2\text{Co}_{0.5}\text{Ir}_{0.5}\text{O}_4$ with a layered K_2NiF_4 -type structure was studied by using hard X-ray absorption and emission spectroscopies. The Co- K and the Ir- L_3 X-ray absorption spectra demonstrate that the Ir⁵⁺ and the Co³⁺ valence states at ambient conditions are not affected by pressure. The Co $K\beta$ emission spectra, on the other hand, revealed a gradual spin state transition of Co³⁺ ions from a high-spin ($S = 2$) state at ambient pressure to a complete low-spin state ($S = 0$) at 40 GPa without crossing the intermediate spin state ($S = 1$). This can be well understood from our calculated phase diagram in which we consider the energies of the low spin, intermediate spin and high spin states of Co³⁺ ions as a function of the anisotropic distortion of the octahedral local coordination in the layered oxide. We infer that a short in-plane Co-O bond length ($< 1.90 \text{ \AA}$) as well as a very large ratio of $\text{Co-O}_{\text{apex}}/\text{Co-O}_{\text{in-plane}}$ is needed to stabilize the IS Co³⁺, a situation which is rarely met in reality.

Layered perovskites A_2BO_4 with a K_2NiF_4 -type structure have been intensively investigated owing to their unique properties, such as high-temperature superconductivity in cuprates, spin-triplet superconductivity in ruthenates, spin/charge stripes in nickelates and manganites¹. Recently, Sr_2IrO_4 with low-spin (LS) Ir⁴⁺ has attracted much attention because of the insulating behavior resulting from the strong spin-orbit interaction^{2,3}, while Sr_2CoO_4 exhibits a metallic behavior because of its intermediate-spin (IS) Co³⁺ coming from both the negative charge-transfer energy and the tetragonal distortion⁴⁻¹⁰. In $\text{La}_{2-x}\text{Sr}_x\text{CoO}_4$, the CoO_6 octahedron has an elongated distortion, and thus the IS Co³⁺ state might be stabilized owing to the single occupation in the e_g levels. Therefore, the spin state of the Co³⁺ ions in $\text{La}_{2-x}\text{Sr}_x\text{CoO}_4$ has been controversially discussed as a pure IS state or alternatively as a mixture of high spin (HS) Co³⁺ and low-spin (LS) Co³⁺¹¹⁻¹⁶. There are also conflicting results in the pressure-driven spin crossover of Co³⁺ ion in the layered compound $\text{Sr}_2\text{CoO}_3\text{F}$ with the K_2NiF_4 -type structure¹⁷. First principle calculations predicted the HS state at ambient pressure and the IS state under high pressure¹⁸, while Co $K\beta$ emission experiments suggested a complete HS-LS transition at 12 GPa without through an IS state¹⁹. Therefore, the presence of the IS Co³⁺ is still under fierce debate.

The hybrid Co/Ir solid-state oxide $\text{Sr}_2\text{Ir}_{2-x}\text{Co}_x\text{O}_4$ system might show unusual electronic and magnetic structures considering the presence of strong intra-atomic multiplet interactions for the localized Co 3d electrons and a large spin-orbit coupling for the delocalized Ir 5d electrons. As indicated by a previous study, the substitution of Ti, Fe, and Co for Ir in Sr_2IrO_4 induces a reduction of the magnetic susceptibility as well as an enhancement of the effective paramagnetic moment for samples with Co and Fe together with a suppression of the weak ferromagnetic ordering²⁰. On the other hand, substituting Mn for Ir results in the reordering and flipping of the spins

¹National Synchrotron Radiation Research Center, Hsinchu, 30076, Taiwan. ²Max Planck Institute for Chemical Physics of Solids, Dresden, D-01187, Germany. ³Karlsruhe Institute of Technology (KIT), Institute for Applied Materials (IAM), Eggenstein-Leopoldshafen, D-76344, Germany. ⁴Institute for Complex Materials, IFW Dresden, Dresden, D-01069, Germany. ⁵Department of Quantum Matter, ADSM, Hiroshima University, Higashi-Hiroshima, 739-8530, Japan. Correspondence and requests for materials should be addressed to H.-J.L. (email: hjlin@nsrrc.org.tw) or J.-M.C. (email: jmchen@nsrrc.org.tw)

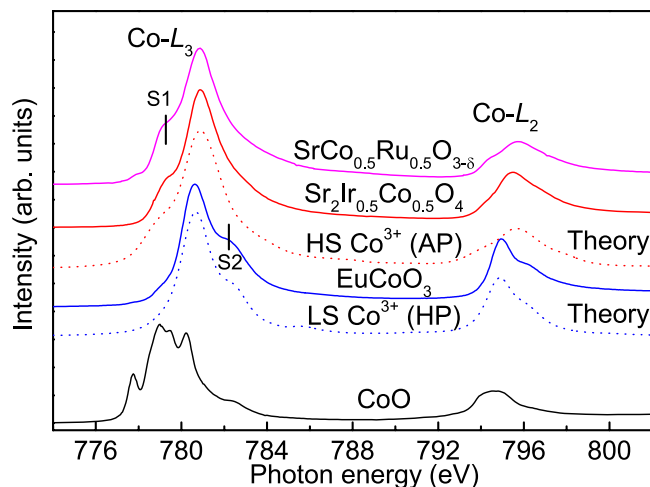


Figure 1. Co- $L_{2,3}$ absorption spectra of $\text{Sr}_2\text{Co}_{0.5}\text{Ir}_{0.5}\text{O}_4$ together with EuCoO_3 as a LS- Co^{3+} ref. 24, $\text{SrCo}_{0.5}\text{Ru}_{0.5}\text{O}_{3-\delta}$ as a HS- Co^{3+} ref. 29, and CoO as a HS- Co^{2+} reference. The theoretical spectra of HS Co^{3+} below $\text{Sr}_2\text{Co}_{0.5}\text{Ir}_{0.5}\text{O}_4$ and LS Co^{3+} below EuCoO_3 are also included for comparison.

as well as a decrease of the magnetic ordering temperature²¹. Co in $\text{Sr}_2\text{Ir}_{1-x}\text{Co}_x\text{O}_4$ is proposed to be in 4+ valence state for Co concentrations up to 30%, while the effective magnetic moment ($4.69 \mu_B$) falls in between what is expected for IS Co^{4+} ($3.87 \mu_B$) and high spin (HS) Co^{4+} ($5.92 \mu_B$)²⁰. However, a later theoretical study proposed the presence of a charge-spin-orbital state in Fe- or Co-doped Sr_2IrO_4 with HS Fe^{3+} and HS Co^{3+} instead of IS Fe^{4+} and IS Co^{4+} ²². The spin state degree of freedom of Co results from subtle balance between crystal field splitting and Hund's rule exchange energy. Pure Low-spin (LS) Co^{3+} is well known, such as LiCoO_2 , NaCoO_2 , and EuCoO_3 , while pure high-spin (HS) Co^{3+} exists only in systems with the relatively weak crystal field like $\text{YBa}_2\text{Co}_4\text{O}_7$ with CoO_4 tetrahedrons²³ and $\text{Sr}_2\text{CoO}_3\text{Cl}$ with CoO_5 pyramids²⁴. The HS Co^{3+} with CoO_6 symmetry in cobalt oxides was only found in the system with a mixture of HS and LS like LaCoO_3 ²⁵ or in the system with oxygen deficiency such as $\text{GdBaCo}_2\text{O}_{5.5}$ ²⁶. Considering that Sr_2IrO_4 has relatively large lattice parameters ($\text{Ir-O}_{\text{in-plane}} = 1.9832 \text{ \AA}$)²⁷, it is expected that the Co^{3+} ions doped in Sr_2IrO_4 would be in a pure HS state owing to the weak crystal field. However, pressure dependence of crystal-structure study on $\text{Sr}_2\text{Co}_{0.5}\text{Ir}_{0.5}\text{O}_4$ has shown a sharp increase of the c/a ratio with pressures up to 10 GPa²⁸. This increase in the tetragonal distortion should favor the IS Co^{3+} state. Furthermore, $\text{Sr}_2\text{Co}_{0.5}\text{Ir}_{0.5}\text{O}_4$ exhibits a negative Weiss constant, indicating a dominant antiferromagnetic interaction in this system²⁸, which might be related to the spin state of Co. In this work, we have investigated the relation between the Co-O bond lengths and the spin states of Co^{3+} ions in $\text{Sr}_2\text{Co}_{0.5}\text{Ir}_{0.5}\text{O}_4$ under external pressures. We have drawn a phase diagram of the spin state of a Co^{3+} ion as a function of the anisotropic Co-O bond lengths.

Results

Co- $L_{2,3}$ X-ray absorption. The Co- $L_{2,3}$ XAS spectrum of $\text{Sr}_2\text{Co}_{0.5}\text{Ir}_{0.5}\text{O}_4$ is presented in Fig. 1 together with those of EuCoO_3 as a LS- Co^{3+} reference, $\text{SrCo}_{0.5}\text{Ru}_{0.5}\text{O}_{3-\delta}$ as a HS- Co^{3+} reference, and CoO as a high-spin (HS) Co^{2+} ^{24,29}. One can see that the center of gravity of the L_3 white line of $\text{Sr}_2\text{Co}_{0.5}\text{Ir}_{0.5}\text{O}_4$ (red line) is at a higher photon energy as compared to that of CoO , while it is similar to that of EuCoO_3 and $\text{SrCo}_{0.5}\text{Ru}_{0.5}\text{O}_{3-\delta}$. This establishes that the Co in $\text{Sr}_2\text{Co}_{0.5}\text{Ir}_{0.5}\text{O}_4$ is trivalent, different from the parent compound Sr_2CoO_4 with Co^{4+} . Moreover, the line shape of the $\text{Sr}_2\text{Co}_{0.5}\text{Ir}_{0.5}\text{O}_4$ spectrum is very different from that of EuCoO_3 , implying a different local electronic structure. As shown in previous studies, the presence of the low-energy shoulder S1 at the Co^{3+} L_3 edge is characteristic for the high-spin state, while the high-energy shoulder S2 is indicative for the low-spin state^{24,29}. The similarity between $\text{Sr}_2\text{Co}_{0.5}\text{Ir}_{0.5}\text{O}_4$ and $\text{SrCo}_{0.5}\text{Ru}_{0.5}\text{O}_{3-\delta}$ also shows the same spin state, namely HS. To further confirm HS Co^{3+} in $\text{Sr}_2\text{Co}_{0.5}\text{Ir}_{0.5}\text{O}_4$, we performed the configuration-interaction cluster calculations including the full atomic multiplet, and the crystal field interactions, as well as the hybridization between the Co and oxygen ions according to Harrison's prescription^{30,31}. The parameter values are listed in ref. 32. The theoretical HS Co^{3+} spectrum was plotted below $\text{Sr}_2\text{Co}_{0.5}\text{Ir}_{0.5}\text{O}_4$. One can observe that the HS- Co^{3+} scenario nicely reproduces all features of the experimental spectrum, further demonstrating the HS Co^{3+} ground state in this system. We would like to note that the 3+ valence of the Co is fully consistent with the finding of the 5+ valence of the Ir ion as demonstrated in the previous study by the Ir- L_3 XAS spectrum²⁸.

Co-K X-ray absorption under pressure. We now investigate the Co spin state as a function of pressure using hard X-rays. The spin state can be determined also by the Co-K XAS spectra, since different spin states possess distinct electronic structures. The Co-K XAS spectra at ambient pressure and at 43 GPa are shown in Fig. 2. The XAS spectra contain two broad features in the pre-edge region around 7710 eV, and one intense absorption peak around 7725 eV. The main peak can be attributed to the dipole transition from the Co 1s core level to the Co 4p unoccupied states, while the pre-edge structures can be assigned to transitions from the Co 1s to the Co 3d t_{2g} and e_g levels owing to the hybridization between Co 3d and 4p states³³. As shown in the inset of Fig. 2, one observes a spectral weight transfer with pressure: the low-energy feature P1 loses its spectral intensity, while

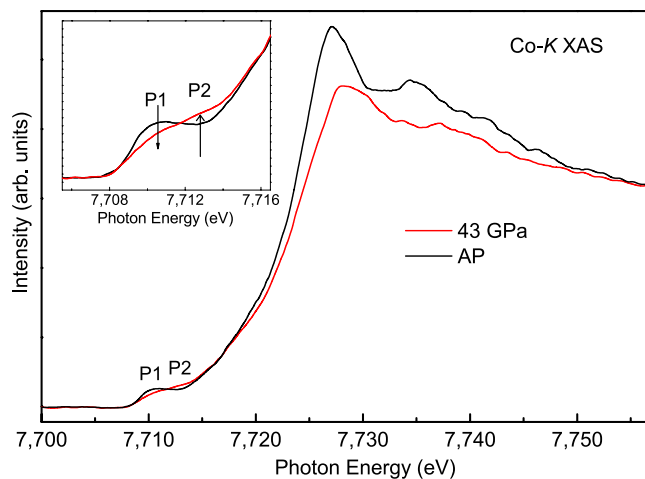


Figure 2. The Co-K PFY XAS spectra of $\text{Sr}_2\text{Co}_{0.5}\text{Ir}_{0.5}\text{O}_4$ at ambient pressure and 43 GPa.

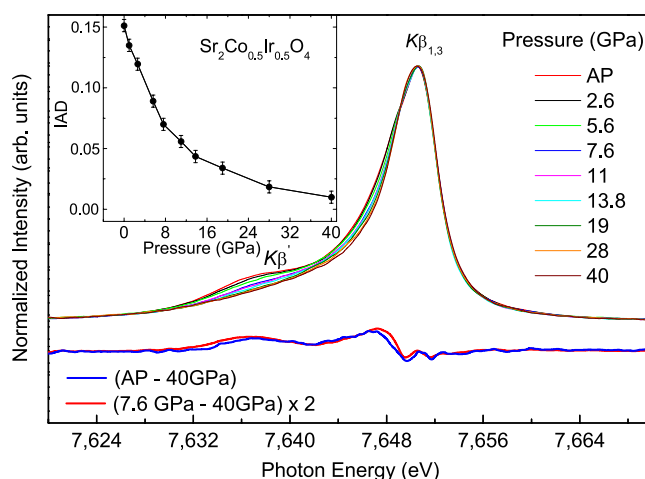


Figure 3. Co $K\beta$ X-ray emission spectra (XES) of $\text{Sr}_2\text{Co}_{0.5}\text{Ir}_{0.5}\text{O}_4$ and difference spectra of Co $K\beta$ emissions between ambient pressure (AP) and 40 GPa (blue line) and between 7.6 and 40 GPa (red line). Inset: Integrated absolute difference (IAD) as a function of pressure for $\text{Sr}_2\text{Co}_{0.5}\text{Ir}_{0.5}\text{O}_4$.

the feature P2 gains its spectral intensity. As indicated by the charge-transfer multiplet calculation in an earlier study³⁴, the LS state has only one single peak in the pre-edge range, while both the IS and HS states possess two features because of the accessible t_{2g} levels in the higher spin states. Since the IS and HS states only have relatively small line shape differences, the strong spectral change implies the increase of the LS content with pressure³⁴. Moreover, the raising edge is also shifted to higher photon energies with pressure. This shift is consistent with the spin state transition from the HS Co^{3+} to LS Co^{3+} , since the latter has a larger band gap. All this is consistent with the findings of the temperature-dependence Co-K XAS studies on LaCoO_3 and $(\text{Pr}_{0.7}\text{Sm}_{0.3})_{0.7}\text{Ca}_{0.3}\text{CoO}_3$ ^{34,35}, in which the Co-K absorption edge of the low spin Co^{3+} at the low temperature is at higher photon energies compared to that of the higher spin Co^{3+} .

Co-KX-ray emission under pressure. To identify the pressure-induced spin state transition of HS- Co^{3+} , we have collected the Co- $K\beta$ emission spectra of $\text{Sr}_2\text{Co}_{0.5}\text{Ir}_{0.5}\text{O}_4$ in the pressure range between ambient pressure and 40 GPa as shown in Fig. 3. The ambient-pressure Co $K\beta$ emission spectrum represents a main peak located at $\sim 7,650$ eV corresponding to the $K\beta_{1,3}$ line, and a pronounced satellite peak at $\sim 7,637$ eV corresponding to the $K\beta'$ line. This line shape is typical for the HS- Co^{3+} state, as obtained in the compounds with HS- Co^{3+} like $\text{SrCo}_{0.5}\text{Ru}_{0.5}\text{O}_{3.6}$ ²⁹ or LaCoO_3 at high temperature³⁴. The intensity ratio of the low-energy $K\beta'$ line to the main emission $K\beta_{1,3}$ line is proportional to the number of the unpaired electrons in the incomplete 3d shell³⁶ and can be used for an indication of spin states in the material^{29,33-35}. With increasing pressure, the intensity of the low-energy $K\beta'$ line decreases and almost disappears at 40 GPa (Fig. 3). Figure 4 presents the Co $K\beta$ XES data of $\text{Sr}_2\text{Co}_{0.5}\text{Ir}_{0.5}\text{O}_4$ at AP and 40 GPa together with those of $\text{Sr}_2\text{CoO}_3\text{F}$ at 1 GPa (HS) and 17 GPa (LS) as well as those of LaCoO_3 at 17 K (LS) and 803 K (mainly HS)^{19,34}. To compare the intensity ratio of the $K\beta_{1,3}$ line and the $K\beta'$ line, those data are aligned and normalized to the $K\beta_{1,3}$ peak. As shown in Fig. 4, the reduction of the $K\beta'$ spectral weight in $\text{Sr}_2\text{Co}_{0.5}\text{Ir}_{0.5}\text{O}_4$ is the same as that of $\text{Sr}_2\text{CoO}_3\text{F}$ ¹⁹ indicating the complete HS-LS state transition in

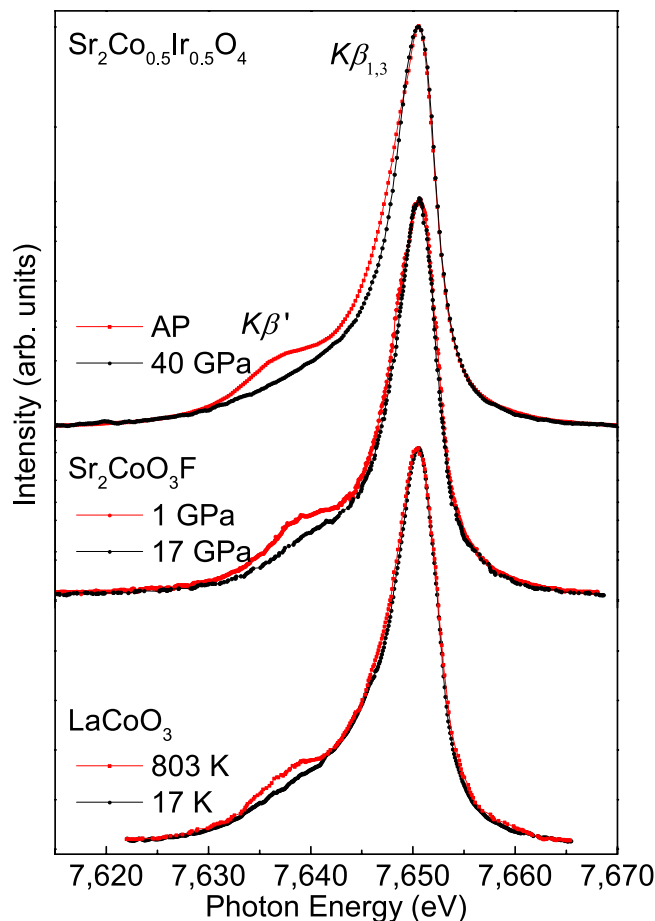


Figure 4. Co $K\beta$ X-ray emission spectra (XES) of $\text{Sr}_2\text{Co}_{0.5}\text{Ir}_{0.5}\text{O}_4$ at ambient pressure (red line) and 40 GPa (blue line) together with those of $\text{Sr}_2\text{CoO}_3\text{F}$ ¹⁹ at 1 GPa (HS) and 17 GPa (LS) and those of LaCoO_3 ³⁴ at 17 K (LS) and 803 K (mainly HS).

$\text{Sr}_2\text{Co}_{0.5}\text{Ir}_{0.5}\text{O}_4$ up to 40 GPa. But the decrease of the $K\beta'$ spectral weight is much larger than that of LaCoO_3 ³⁴ from 803 K to 17 K, since the spin state transition in the latter is not complete in this temperature range. Furthermore, the inset of Fig. 3 presents integrated absolute difference (IAD) as a function of pressure^{33–35}, and the total IAD changes by about 0.14 from ambient pressure to 40 GPa. This value is similar to that of $\text{SrCo}_{0.5}\text{Ru}_{0.5}\text{O}_{3-\delta}$ ²⁹ and consistent with what is expected for a complete HS ($S=2$) to LS ($S=0$) transition³⁷.

At 7.6 GPa, the IAD value of ~ 0.07 corresponds to the change in the spin state $\Delta S=1$, comparing with the value at ambient pressure. Two possible scenarios may satisfy the averaged spin state with $S=1$: either the existence of intermediate spin state of Co^{3+} (IS- Co^{3+} , $S=1$) or a coexistence of equal amounts of HS- Co^{3+} ($S=2$) and LS- Co^{3+} ($S=0$). The presence of IS- Co^{3+} in perovskite-like oxides is a matter of long-time discussions, especially for LaCoO_3 ^{34,38,39} and other rare-earth metal cobaltates⁴⁰. In the case of layered perovskites, the reported results about spin-state crossover of the Co^{3+} ions are also controversial: for example, upon replacement of La^{3+} by the larger Sr^{2+} in $\text{La}_{2-x}\text{Sr}_x\text{CoO}_4$ a drastic change of magnetic and electronic properties was ascribed to a spin-state transition of Co^{3+} from a high-spin to an intermediate-spin⁴¹. On the other hand, spin state transition from the LS- Co^{3+} to HS- Co^{3+} upon the increase of temperature was reported for single crystals of $\text{La}_{2-x}\text{Sr}_x\text{CoO}_4$, based also on susceptibility data analysis¹⁴.

In order to distinguish between two scenarios of possible Co^{3+} spin state in the layered $\text{Sr}_2\text{Co}_{0.5}\text{Ir}_{0.5}\text{O}_4$ at 7.6 GPa with the total spin state $S=1$, namely a mixture of HS- Co^{3+} and LS- Co^{3+} and pure IS- Co^{3+} , we drew the difference spectra of Co- $K\beta$ emissions obtained between ambient pressure (AP) and 40 GPa (red line) as well as between 7.6 GPa and 40 GPa (blue line) shown in Fig. 3 (below the X-ray emission spectra). The red line corresponds to the change in the spin number $\Delta S=2$, while the blue line describes the change in the spin number $\Delta S=1$. These two difference spectra are almost identical apart from the scale factor of 2, used for the blue line, what is consequent with the scenario “1:1 mixture of HS- Co^{3+} and LS- Co^{3+} at 7.6 GPa”. Thus, the difference of the spectra does not show any sign for new features which would be expected for the presence of an intermediate spin state of Co^{3+} . Therefore, a continuous spin state transition from HS- Co^{3+} to LS- Co^{3+} under pressures in $\text{Sr}_2\text{Co}_{0.5}\text{Ir}_{0.5}\text{O}_4$ can be verified. Note that in contrast to the nearly monotonous change of the IAD of $\text{SrCo}_{0.5}\text{Ru}_{0.5}\text{O}_3$ with the pressure²⁹, in the case of $\text{Sr}_2\text{Co}_{0.5}\text{Ir}_{0.5}\text{O}_4$ the IAD decreases fast up to 10–12 GPa following by slower decreasing at higher pressures. It might be related to the anisotropy compression of $\text{Sr}_2\text{Co}_{0.5}\text{Ir}_{0.5}\text{O}_4$ observed in the previous study²⁸.

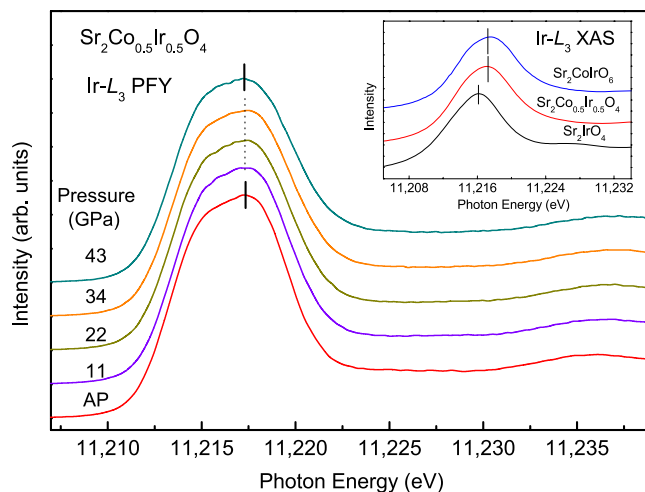


Figure 5. Pressure-dependence of the Ir- L_3 PFY spectra of $\text{Sr}_2\text{Co}_{0.5}\text{Ir}_{0.5}\text{O}_4$. Inset shows the Ir- L_3 XAS spectra of $\text{Sr}_2\text{Co}_{0.5}\text{Ir}_{0.5}\text{O}_4$, Sr_2IrO_4 as an Ir^{4+} reference and of $\text{Sr}_2\text{CoIrO}_6$ as an Ir^{5+} reference for comparison.

Ir- L_3 X-ray absorption under pressure. At this point we also would like to know whether the reduction of Co spin moment under pressure results from a change of the Co configuration from HS Co^{3+} ($S=2$) to LS Co^{4+} ($S=1/2$) accompanying with a change of the Ir valence state from $5+$ to $4+$. For this purpose, we measured the partial fluorescence spectra at the Ir- L_3 edge of $\text{Sr}_2\text{Co}_{0.5}\text{Ir}_{0.5}\text{O}_4$ under pressures up to 43 GPa. As shown in Fig. 5, from bottom to top, there is no energy shift of the Ir- L_3 PFY XAS spectra with the external pressures from AP to 43 GPa, indicating that the Ir valence remains $5+$, since a reduction of Ir valence state would lead to an energy shift to lower photon energies. As shown in inset of Fig. 5, the Ir- L_3 XAS spectrum of $\text{Sr}_2\text{Co}_{0.5}\text{Ir}_{0.5}\text{O}_4$ measured in a transmission mode at ambient pressure is at higher photon energies compared with that of Sr_2IrO_4 with Ir^{4+} , but locates at nearly the same photon energy as that of $\text{Sr}_2\text{CoIrO}_6$ with Ir^{5+} ⁴². Thus, we reaffirm that the decrease of the cobalt moment under pressure is solely due to a gradual spin state transition of Co^{3+} ions without any change in the valence state of the Co ions and also reaffirm the Ir^{5+} valence state, fulfilling the charge balance requirement for $\text{Co}^{3+}/\text{Ir}^{5+}$ valence states in the studied $\text{Sr}_2\text{Co}_{0.5}\text{Ir}_{0.5}\text{O}_4$ sample.

Discussion

Using the element selective Co- K EXAFS (extended X-ray absorption fine structure) we can determine Co-O distance at ambient pressure²⁸. If we assumed that the pressure-induced variation of the Co-O bond lengths would be proportional to the variation of the lattice parameters, then we estimated Co-O bond lengths as a function of pressure from the lattice parameters obtained in the previous high pressure study²⁸, as presented in Fig. 6(a). Please note that under external pressures, a CoO_6 octahedron might rotate in the basal plane, as observed in the study on Sr_2RuO_4 and Sr_2IrO_4 ²⁷. Therefore, the reduction of the in-plane Co-O bond distances might be overestimated. However, our theoretical predication of the total energies of HS, LS and IS states as a function of in-plane and out-plane Co-O distances response to external pressure in general is still valid. One can see that the in-plane Co-O distance ($\text{Co-O}_{\text{in-plane}}$ blue squares) reduces faster than that for the apex ($\text{Co-O}_{\text{apex}}$ red circles) up to 10 GPa, namely $\text{Co-O}_{\text{apex}}/\text{Co-O}_{\text{in-plane}}$ (black line) increases with high pressure²⁶. One would expect that the IS ground state of Co^{3+} ion with one electron in e_g orbital could be stabilized under high pressure as the tetragonal distortion increases with high pressure. It is puzzled, however, our above Co $K\beta$ X-ray emission spectra indicate a pressure-induced spin state transition from the HS state to the LS state without crossing the IS state.

To understand above experimental observation on the spin state transition, we have calculated the total energies of the LS, IS, and HS states as a function of pressure by taking the estimated $\text{Co-O}_{\text{apex}}$ bond length and $\text{Co-O}_{\text{in-plane}}$ bond length into account using the configuration-interaction cluster calculation. The hybridization part is obtained according to the Harrison's rules and the ionic crystal field is calculated as the Madelung potential. The factor of the Madelung potential can be determined because the HS and LS states are degenerated at 7.6 GPa, as observed in the Co $K\beta$ X-ray emission spectra. The results are presented in Fig. 6(b). One can see in Fig. 6(b) that at ambient pressure, the ground state is the HS state consistent with the experimental $\text{Co-L}_{2,3}$ XAS and Co $K\beta$ X-ray emission results. Under external pressures up to 7.6 GPa, the LS and IS states gain more energies than the HS state due to the increase of $10Dq$ because of a reduction of the Co-O bond lengths and to the enhancement of the e_g splitting (Δe_g) from an increase of $\text{Co-O}_{\text{apex}}/\text{Co-O}_{\text{in-plane}}$, respectively. However, the energy gain of the LS Co^{3+} state ($-24Dq$) overwhelms that of the IS Co^{3+} state ($-14Dq-0.5\Delta e_g$). Therefore, as presented in Fig. 6(b), the LS state becomes the ground state when $\text{Co-O}_{\text{apex}}/\text{Co-O}_{\text{in-plane}}$ is larger than 1.065 at the pressure about 7.6 GPa. When the external pressure is larger than 9.7 GPa, the LS state becomes even more stable against the HS and the IS owing to the further increase in $10Dq$ and also a reduction of Δe_g as $\text{Co-O}_{\text{apex}}/\text{Co-O}_{\text{in-plane}}$ decreases. As shown in Fig. 6(b), the IS state will never be the ground state under the pressure performed for the layered $\text{Sr}_2\text{Co}_{0.5}\text{Ir}_{0.5}\text{O}_4$, and thus one might wonder what is the condition to stabilize the IS state as a ground state for Co^{3+} .

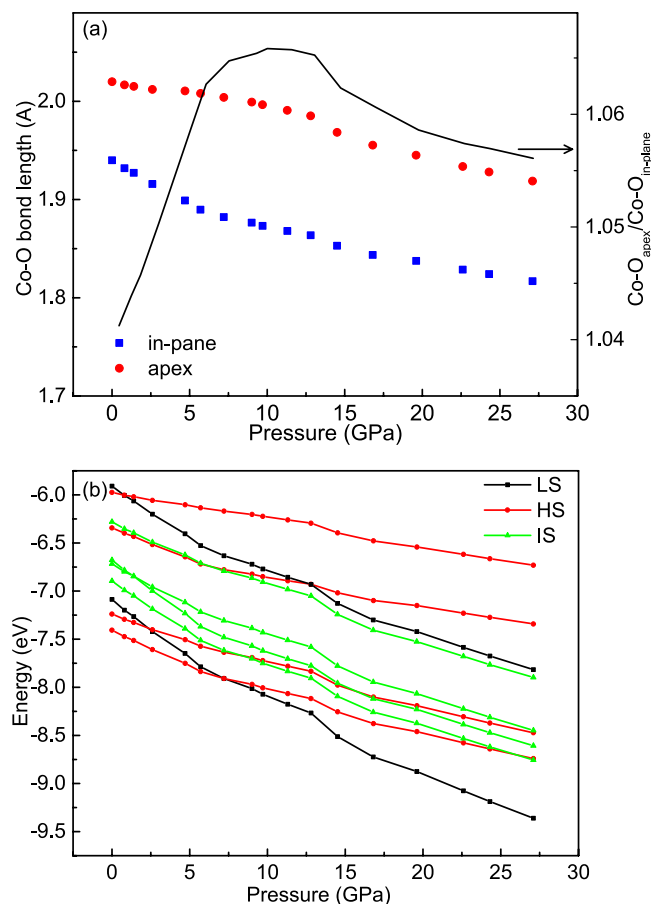


Figure 6. (a) Co-O_{apex} bond length (red circles) and Co-O_{in-plane} bond length (blue squares) as well as the ratio Co-O_{apex}/Co-O_{in-plane} (black line) as a function of the external pressure derived from ref. 28. Note that the reduction of the in-plane Co-O bond distance might be overestimated due to the possible rotation of the CoO₆ octahedron. (b) The energy diagram of three spin states as a function of the pressure using Co-O bond lengths in (a).

In order to scrutinize the stable conditions for the IS Co³⁺ state in the layered structure, we have calculated the phase diagram of the ground state as a function of Co-O_{apex} and Co-O_{in-plane}. The phase diagram shown in Fig. 7 indicates that the strong elongated tetragonal distortion indeed could stabilize the IS state if the in-plane Co-O distance (Co-O_{in-plane}) is rather short and ratio of Co-O_{apex}/Co-O_{in-plane} is quite large. In other words, the short in-plane Co-O bond length as well as the strong tetragonal distortion favors IS. However, if the Co-O_{in-plane} is larger than 1.90 Å, the IS state will be hardly stabilized. Therefore, IS cannot be stabilized by heating the sample as illustrated with the blue line where the Co-O distance increases with temperature by keeping the ratio of Co-O_{apex}/Co-O_{in-plane} at room temperature in Fig. 7. On the other hand, the presence of the IS ground state might be possible in TlSr₂CoO₅, where one of two Co³⁺ sites at low temperatures (O-phase) has a small value of the Co-O_{in-plane} = 1.79 Å and Co-O_{apex} = 2.19 Å, presented as a green circle in Fig. 7^{43,44}. Besides, the Co-O bond lengths (magenta circles) in Sr₂Co_{0.5}Ir_{0.5}O₄ under external pressures are plotted in this phase diagram. One can see that the ground state of Co³⁺ ion in Sr₂Co_{0.5}Ir_{0.5}O₄ has a stable HS state and is transformed to the LS state with the external pressures without crossing the IS state (magenta circles). On the other hand, the Co-O bond distance of LaCoO₃ is reduced from 1.9329 Å to 1.888 Å crossing a mixed HS/LS state to a pure LS state with pressure³⁹. The mixed spin state of LaCoO₃ is due to the much shorter Co-O bond distance, close to the boundary of the HS and LS, as compared with that of Sr₂Co_{0.5}Ir_{0.5}O₄ (Co-O_{in-plane} = 1.967 Å and Co-O_{apex} = 2.020 Å)²⁸.

Conclusion

We have studied the valence state and spin state transition of Co ion under external pressures in a hybrid 3d-5d transition metals solid-state oxide Sr₂Co_{0.5}Ir_{0.5}O₄ using hard X-ray absorption and Co-Kβ emission spectroscopies. The high spin state of Co³⁺ ions found at ambient pressure exhibits a complete spin state transition to the low-spin state up to 40 GPa without crossing the intermediate-spin state, while the valence state of Ir⁵⁺ ions remains unchanged. At external pressures below 9.7 GPa, the fast increase of the ratio of Co-O_{apex}/Co-O_{in-plane} does not stabilize the IS state but the LS state instead owing to a rapid increase of 10Dq overwhelming the Jahn-Teller distortion of the e_g orbitals. Above 9.7 GPa, the LS state becomes even more stable due to the decrease of the ratio of Co-O_{apex}/Co-O_{in-plane}. To determine the condition for stabilizing a possible intermediate-spin ground state in such a layered oxide, we have compared the energies of the three different spin states of Co³⁺ ions

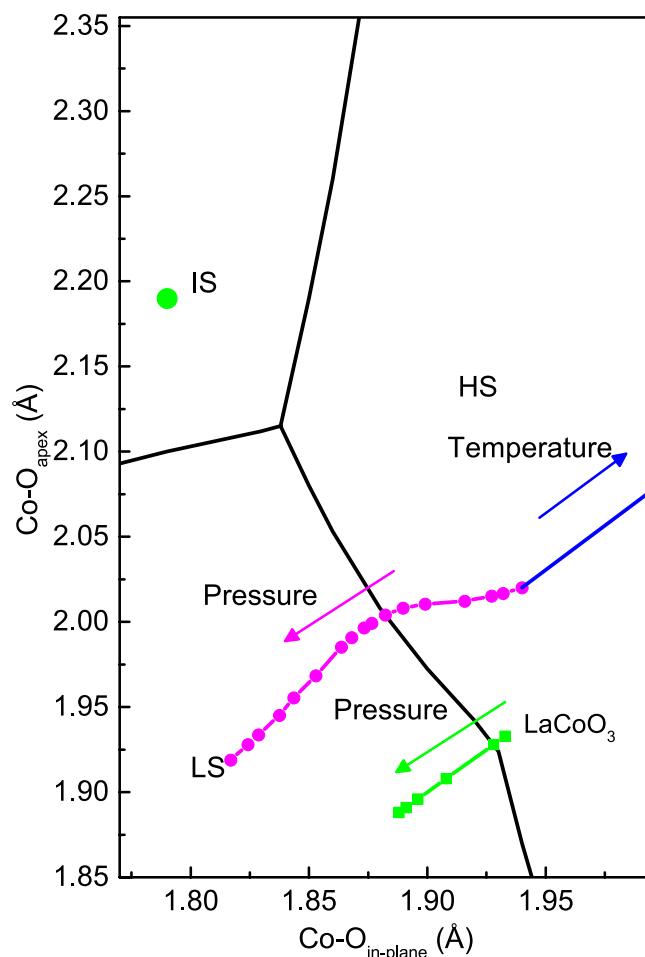


Figure 7. The phase diagram of the ground state of Co^{3+} as a function of Co-O bond lengths. The magenta circles are the Co-O bond lengths of $\text{Sr}_2\text{Co}_{0.5}\text{Ir}_{0.5}\text{O}_4$ estimated from ref. 28 and the blue line refers to an increase of its Co-O distance with temperature by keeping the ratio of $\text{Co-O}_{\text{apex}}/\text{Co-O}_{\text{in-plane}}$ at room temperature. The green circle is those of one of two Co^{3+} sites in the O-phase in $\text{TlSr}_2\text{CoO}_5$ ⁴³. The green line represents the Co-O distances of LaCoO_3 ³⁹ with pressure.

as a function of bond lengths. These results have been plotted in a phase diagram and a stable IS state can only be found when the in-plane Co bond length is substantially shorter than the $\text{Co-O}_{\text{apex}}$ bond length.

Methods

Sample synthesis. The layered polycrystalline $\text{Sr}_2\text{Co}_{0.5}\text{Ir}_{0.5}\text{O}_4$ was synthesized from solid state reaction as described previously²⁸. The purity and unit cell parameters were determined by X-ray powder diffraction (XPD). $\text{Sr}_2\text{Co}_{0.5}\text{Ir}_{0.5}\text{O}_4$ is more insulating than Sr_2IrO_4 ⁴⁵, as indicated by the resistivity data in Fig. S1 in the Supplementary Information.

X-Ray spectroscopy. The $\text{Co-L}_{2,3}$ X-ray absorption spectroscopy (XAS) measurements were recorded at the BL11A beam line of the National Synchrotron Radiation Research Center (NSRRC) in Taiwan. Clean sample surfaces were obtained by cleaving pelletized samples *in situ* in an ultra-high vacuum chamber with a pressure of 10^{-10} mbar range. The $\text{Co-L}_{2,3}$ spectra were collected at room temperature using total electron yield mode (TEY) with an energy resolution of about 0.3 eV. The high-pressure Co-K and Ir-L_3 partial-fluorescence-yield (PFY) XAS spectra and $\text{Co K}\beta$ X-ray emission spectra were obtained at the Taiwan inelastic X-ray scattering BL12XU beamline at SPring-8 in Japan. A Mao-Bell diamond anvil cell with a Be gasket was used for the high-pressure experiment. Silicone oil served as a medium to transmit pressure. The applied pressure in the diamond anvil cell was measured through the Raman line shift of ruby luminescence before and after each spectral collection. The $\text{Co K}\beta$ X-ray emission spectra were collected at 90° from the incident X-ray and analyzed with a spectrometer (Johann type) equipped with a spherically bent Ge(444) crystal and Si(553) (radius 1 m), respectively, arranged on a horizontal plane in a Rowland-circle geometry.

References

1. Imada, M., Fujimori, A. & Tokura, Y. Metal-insulator transitions. *Rev. Mod. Phys.* **70**, 1039–1263 (1998).
2. Kim, B. J. *et al.* Novel Jeff=1/2 Mott State Induced by Relativistic Spin-Orbit Coupling in Sr_2IrO_4 . *Phys. Rev. Lett.* **101**, 076402 (2008).

3. Kim, B. J. *et al.* Phase-Sensitive Observation of a Spin-Orbital Mott State in Sr₂IrO₄. *Science* **323**, 1329–1332 (2009).
4. Matsuno, J. *et al.* Metallic Ferromagnet with Square-Lattice CoO₂ Sheets. *Phys. Rev. Lett.* **93**, 167202 (2004).
5. Wang, X. L. & Takayama-Muromachi, E. Magnetic and transport properties of the layered perovskite system Sr_{2-y}Y_yCoO₄ (0 ≤ y ≤ 1). *Phys. Rev. B* **72**, 064401 (2005).
6. Matsuno, J. *et al.* Novel metallic ferromagnet Sr₂CoO₄. *Thin Solid Films* **486**, 113–116 (2005).
7. Matsuno, J., Okimoto, Y., Kawasaki, M. & Tokura, Y. Variation of the Electronic Structure in Systematically Synthesized Sr₂MO₄ (M = Ti, V, Cr, Mn, and Co). *Phys. Rev. Lett.* **95**, 176404 (2005).
8. Lee, K.-W. & Pickett, W. E. Correlation effects in the high formal oxidation-state compound Sr₂CoO₄. *Phys. Rev. B* **73**, 174428 (2006).
9. Pandey, S. K. Correlation induced half-metallicity in a ferromagnetic single-layered compound: Sr₂CoO₄. *Phys. Rev. B* **81**, 035114 (2010).
10. Wu, H. Metal-insulator transition in Sr_{2-y}La_xCoO₄ driven by spin-state transition. *Phys. Rev. B* **86**, 075120 (2012).
11. Shimada, Y., Miyasaka, S., Kumai, R. & Tokura, Y. Semiconducting ferromagnetic states in La_{1-x}Sr_{1+x}CoO₄. *Phys. Rev. B* **73**, 134424 (2006).
12. Chichev, A. V. *et al.* Structural, magnetic, and transport properties of the single-layered perovskites La_{2-x}Sr_xCoO₄ (x = 1.0–1.4). *Phys. Rev. B* **74**, 134414 (2006).
13. Wu, H. High-spin and low-spin mixed state in LaSrCoO₄: An *ab initio* study. *Phys. Rev. B* **81**, 115127 (2010).
14. Hollmann, N. *et al.* Evidence for a temperature-induced spin-state transition of Co³⁺ in La_{2-x}Sr_xCoO₄. *Phys. Rev. B* **83**, 174435 (2011).
15. Merz, M. *et al.* Spin and orbital states in single-layered La_{2-y}Ca_xCoO₄ studied by doping- and temperature-dependent near-edge x-ray absorption fine structure. *Phys. Rev. B* **84**, 014436 (2011).
16. Moritomo, Y., Higashi, K., Matsuda, K. & Nakamura, A. Spin-state transition in layered perovskite cobalt oxides: La_{2-y}Sr_xCoO₄ (0.4 ≤ x ≤ 1.0). *Phys. Rev. B* **55**, R14725–R14728 (1997).
17. Tsujimoto, Y. *et al.* Crystal Structural, Magnetic, and Transport Properties of Layered Cobalt Oxyfluorides, Sr₂CoO_{3+x}F_{1-x} (0 ≤ x ≤ 0.15). *Inorg. Chem.* **51**, 4802–4809 (2012).
18. Ou, X., Fan, F., Li, Z., Wang, H. & Wu, H. Spin-state transition induced half metallicity in a cobaltate from first principles. *Appl. Phys. Lett.* **108**, 092402 (2016).
19. Tsujimoto, Y. *et al.* Crystal Pressure-Driven Spin Crossover Involving Polyhedral Transformation in Layered Perovskite Cobalt Oxyfluoride. *Sci. Rep.* **6**, Article number: 36253 (2016).
20. Gatimu, A. J., Berthelot, R., Muir, S., Sleight, A. W. & Subramanian, M. A. Synthesis and characterization of Sr₂Ir_{1-x}M_xO₄ (M = Ti, Fe, Co) solid solutions. *J. Solid State Chem.* **190**, 257–263 (2012).
21. Calder, S. *et al.* Magnetic structural change of Sr₂IrO₄ upon Mn doping. *Phys. Rev. B* **86**, 220403 (2012).
22. Ou, X. & Wu, H. Coupled charge-spin-orbital state in Fe- or Co-doped Sr₂IrO₄. *Phys. Rev. B* **89**, 035138 (2014).
23. Hollmann, N. *et al.* Electronic and magnetic properties of the kagome systems YBaCo₃O₇ and YBaCo₃MO₇ (M = Al, Fe). *Phys. Rev. B* **80**, 085111 (2009).
24. Hu, Z. *et al.* Different Look at the Spin State of Co³⁺ Ions in a CoO₂ Pyramidal Coordination. *Phys. Rev. Lett.* **92**, 207402 (2004).
25. Haverkort, M. W. *et al.* Spin State Transition in LaCoO₃ Studied Using Soft X-ray Absorption Spectroscopy and Magnetic Circular Dichroism. *Phys. Rev. Lett.* **97**, 176405 (2006).
26. Hu, Z. *et al.* Spin-state order/disorder and metal-insulator transition in GdBaCo₂O_{5.5}: experimental determination of the underlying electronic structure. *New J. Phys.* **14**, 123025 (2012).
27. Huang, Q. *et al.* Neutron Powder Diffraction Study of the Crystal Structures of Sr₂RuO₄ and Sr₂IrO₄ at Room Temperature and at 10 K. *J. Solid State Chem.* **112**, 355 (1994).
28. Mikhailova, D. *et al.* Charge Transfer and Structural Anomaly in Stoichiometric Layered Perovskite Sr₂Co_{0.5}Ir_{0.5}O₄. *Eur. J. Inorg. Chem.* **2017**, 587–595 (2017).
29. Chen, J.-M. *et al.* A Complete High-to-Low spin state Transition of Trivalent Cobalt Ion in Octahedral Symmetry in SrCo_{0.5}Ru_{0.5}O_{3.6}. *J. Am. Chem. Soc.* **136**(4), 1514–1519 (2014).
30. Groot, F. M. F. de X-ray absorption and dichroism of transition metals and their compounds. *J. Electron Spectrosc. Relat. Phenom.* **67**, 529–622 (1994).
31. Tanaka, A. & Jo, T. Resonant 3d, 3p and 3s Photoemission in Transition Metal Oxides Predicted at 2p Threshold. *J. Phys. Soc. Jpn.* **63**, 2788–2807 (1994).
32. Udd = 5.5 eV, Upd = 7.0 eV; Δ = 2.0 eV; The Slater integrals were reduced to 80% of their Hartree-Fock values.
33. Herrero-Martín, J. *et al.* Spin-state transition in Pr_{0.5}Ca_{0.5}CoO₃ analyzed by x-ray absorption and emission spectroscopies. *Phys. Rev. B* **86**, 125106 (2012).
34. Vankó, G., Rueff, J.-P., Mattila, A., Németh, Z. & Shukla, A. Temperature- and pressure-induced spin-state transitions in LaCoO₃. *Phys. Rev. B* **73**, 024424 (2006).
35. Chen, J. M. *et al.* Evolution of spin and valence states of (Pr_{0.7}Sm_{0.3})_{0.7}Ca_{0.3}CoO₃ at high temperature and high pressure. *Phys. Rev. B* **90**, 035107 (2014).
36. Tsutsumi, K., Nakamori, H. & Ichikawa, K. X-ray Mn Kβ emission spectra of manganese oxides and manganates. *Phys. Rev. B* **13**, 929–933 (1976).
37. Oka, K. *et al.* Pressure-Induced Spin-State Transition in BiCoO₃. *J. Am. Chem. Soc.* **132**(27), 9438–9443 (2010).
38. Kozlenko, D. P. *et al.* Temperature- and pressure-driven spin-state transitions in LaCoO₃. *Phys. Rev. B* **75**, 064422 (2007).
39. Vogt, T., Hriljac, J. A., Hyatt, N. C. & Woodward, P. Pressure-induced intermediate-to-low spin state transition in LaCoO₃. *Phys. Rev. B* **67**, 140401 (2003).
40. Baier, J. *et al.* Spin-state transition and metal-insulator transition in La_{1-x}Eu_xCoO₃. *Phys. Rev. B* **71**, 014443 (2005).
41. Cwik, M. The Interplay of Lattice, Spin, and Charge Degrees of Freedom in Layered Cobaltates. Ph.D. Dissertation, Universität of Cologne, Cologne, 2007.
42. Mikhailova, D. *et al.* Oxygen-driven competition between low-dimensional structures of Sr₃CoMO₆ and Sr₃CoMO₇₋₈ with M = Ru, Ir. *Dalton Trans.* **43**, 13883–13891 (2014).
43. Doumerc, J.-P. *et al.* Crystal structure of the thallium strontium cobaltite TlSr₂CoO₅ and its relationship to the electronic properties. *J. Mater. Chem.* **11**, 78–85 (2001).
44. Doumerc, J.-P., Grenier, J.-C., Hagenmuller, P., Pouchard, M. & Villesuzanne, A. Interplay between Local Electronic Configuration and the Occurrence of a Metallic State: An Experimental Approach. *J. Solid State Chem.* **147**, 211–217 (1999).
45. Kini, N. S., Strydom, A. M., Jeevan, H. S., Geibel, C. & Ramakrishnan, S. Transport and thermal properties of weakly ferromagnetic Sr₂IrO₄. *J. Phys.: Condens. Matter* **18**, 8205–8216 (2006).

Acknowledgements

This work is supported by the Ministry of Science and Technology under Grant Nos. MOST 102-2112-M-213 -004 -MY3 and MOST 105-2113-M-213 -005 -MY3 and in Dresden supported by the Deutsche Forschungsgemeinschaft through SFB 1143.

Author Contributions

D.M. prepared the sample in this study. Z.H., C.Y.K., J.M.L., S.C.H., S.A.C., W.S., H.I., N.H., Y.F.L., K.D.T., C.T.C., L.H.T., and J.M.C. conducted the experiments. Y.Y.C., H.J.L., Z.H., and A.T. conducted the cluster calculations. Y.Y.C., H.J.L., Z.H., J.M.C., and L.H.T. wrote the paper. All authors reviewed the manuscript.

Additional Information

Supplementary information accompanies this paper at doi:[10.1038/s41598-017-03950-z](https://doi.org/10.1038/s41598-017-03950-z)

Competing Interests: The authors declare that they have no competing interests.

Publisher's note: Springer Nature remains neutral with regard to jurisdictional claims in published maps and institutional affiliations.



Open Access This article is licensed under a Creative Commons Attribution 4.0 International License, which permits use, sharing, adaptation, distribution and reproduction in any medium or format, as long as you give appropriate credit to the original author(s) and the source, provide a link to the Creative Commons license, and indicate if changes were made. The images or other third party material in this article are included in the article's Creative Commons license, unless indicated otherwise in a credit line to the material. If material is not included in the article's Creative Commons license and your intended use is not permitted by statutory regulation or exceeds the permitted use, you will need to obtain permission directly from the copyright holder. To view a copy of this license, visit <http://creativecommons.org/licenses/by/4.0/>.

© The Author(s) 2017